

Chemical and mechanical treatments to improve the surface properties of shape memory NiTi wires

S. Rossi^{*}, F. Deflorian, A. Pegoretti, D. D'Orazio, S. Gialanella

Dipartimento di Ingegneria dei Materiali e Tecnologie Industriali, Università di Trento and INSTM Research Unit, Via Mesiano 77 38100 Trento, Italy

Received 13 April 2007; accepted in revised form 12 September 2007

Available online 20 September 2007

Abstract

In this paper the results of an experimental study concerning the effect of different surface treatments on NiTi shape memory alloy wires are presented. These treatments were conducted in order to improve the adhesion properties between the NiTi wires and an epoxy resin, acting as the matrix of a composite material.

Mechanical and chemical surface treatments (immersion in acid and alkaline solutions), and different combinations of the above surface preparation procedures were studied.

For the characterisation of the resulting alloy surface conditions electrochemical impedance spectroscopy, polarisation curves and potential versus time measurements were carried out.

The alloy wire/epoxy matrix adhesion was characterised through pull out tests. The results proved that all adopted treatments can remarkably influence the electrochemical properties of the wires. The acid treatments favour the formation of a surface passivation layer, while the alkaline treatments are effective in producing a rougher surface morphology. Moreover, these basic treatments significantly reduce corrosion resistance of the alloys, another material property that has been incidentally investigated in the present context. The main effect of the mechanical surface treatment, consisting in abrading the alloy wires using an emery paper, was to increase the homogeneity of surface roughness.

From the experimental results clear indications on the most promising surface treatments can be inferred.

© 2007 Elsevier B.V. All rights reserved.

Keywords: Shape memory materials; Surface treatments; NiTi alloys; Composite materials; Pull-out test

1. Introduction

Shape memory alloys (SMAs), in view of their peculiar functional properties, are becoming increasingly interesting over recent years for several applications [1].

In view of their peculiar features and functional properties, SMAs are used for actuators, fittings, biomedical applications, clamping systems, etc. Another field, which is disclosing interesting perspectives, is the use of SMA wires as reinforcing and functionalising fibres in polymer matrix composites [2,3]. SMAs are definitely attractive candidates to be added to composites, as they exhibit properties and behaviours, like actuation capability, superelastic response and self-recovery,

damping capacity [4], that can extend the application fields of these materials. Several papers report on the use of SMAs in composites, for the control of the component shape and residual internal stress [2].

One of the most widely investigated alloy system, i.e., NiTi, displays in addition to the typical shape memory phenomenology an excellent corrosion resistance in different electrolytes [5,6]. The high concentration of titanium in these alloys renders all processing and manufacturing steps, namely those carried out at high temperatures, particularly critical as concerns the risk of oxidation and, in general, oxygen contamination. Indeed, the formation of a surface oxide layer, e.g., TiO₂, may change the temperature range for the phase transition, on which the relevant aspects of the shape memory effect are based and that is very sensitive to the actual alloy composition [1]. The temperature shift observed in these cases can be ascribed to nickel surface enrichment, as this element is contributing to a lower

^{*} Corresponding author. Fax: +39 0461881977.

E-mail address: Stefano.Rossi@ing.unitn.it (S. Rossi).

extent than titanium to the formation of the outer oxide layer [1]. Similar modifications in the transition temperatures may be also induced by thermomechanical treatments, possibly involved with the processing of the SMA components, that can be subsequently recovered by suitable anneals [7,8]. All these aspects are to be considered as concerns both composite processing and application.

Moreover, in view of the final applications, the adhesion properties of the alloy-matrix interface have been evaluated [3,4,9,10], with particular reference to the influence of surface topography and surface finishing [11]. An optimised alloy-matrix interface is particularly important to fully exploit the potentials and the properties of shape memory materials [6]. Too a weak adhesion between fibre and polymeric matrix prevents or hinders an effective stress transmission. Moreover, partial or complete detachment of the alloy from the matrix may result in the loss of composite functionality.

The interface stability against corrosion is another important issue, as the formation of corrosion products at the fibre-matrix interface can unpredictably reduce the adhesion strength.

For these reasons several research efforts have been devoted to developing methods for modifying the surface of SMA fibres, in order to improve their corrosion behaviour and, thereby, adhesion to a polymer matrix [12]. As concerns native oxides, it should be mentioned that, although they usually enhance the adhesion strength between fibre and matrix because of their higher roughness [13], on the other hand, they may also show two drawbacks: reduction of the alloy volume that displays shape memory effect and debonding from the matrix, when a de-cohesive failure of the oxide occurs.

Other studies have considered the influence on interface adhesion of surfactants, silanes, titanates or of complex surface finishing processes [14,15]. Laser [16,17], excimer laser [18] and laser gas nitriding [19–22] treatments, strain-hardening and chemical passivation treatments [23] are alternative routes that have been explored over the years. The improvements descending from laser treatments are explained in terms of homogenisation of surface morphology and composition induced by melting. A positive effect has been also ascribed to surface hardening due to nitrogen incorporation in the native oxide layer, that for this reason results comparatively thicker [18].

Other treatments, that have been investigated to improve surface properties of NiTi materials are plasma immersion and ion implantation [24–30]. Mechanical abrasion was also considered and an improvement in the adhesion properties was generally observed [31,32].

Particularly attractive are chemical passivation treatments, that can be easily carried out by just dipping the SMA materials into a nitric acid solution, which induces the formation of a well protective titanium oxide layer, that remarkably improves corrosion resistance [33,34].

With electrolytic procedures it is possible to remove the heat-affected zones, modified by thermal treatments, even in small, finely structured components [34].

Chen et al. [33] have developed a two step treatment (nitric acid followed by a basic solution), which renders the oxide layer more porous.

We present herewith the results of a systematic investigation on several surface treatments conducted on two NiTi alloy wires with the intention of achieving an general improvement of their adhesion to a polymer matrix. The two alloys have been selected so that at room temperature in each of them one of the two polymorphs of the NiTi intermetallic is stable.

Surface treatments having effects on both chemical composition of the surface reaction products and on the topography of the alloy surface itself have been selected. The interplay between surface morphology and corrosion resistance has been also characterised using electrochemical and microscopy techniques.

The surface treated wires were subsequently embedded in a polymeric resin in order to check their adhesion using pull out test. In this respect the proposed approach represents a novel methodology to improve the performances of SMA functionalised composite materials.

2. Experimental

In the present study, NiTi wires with a diameter of 0.8 mm, made of two commercial NiTi alloys purchased from Memory Metalle GmbH (D), have been investigated.

The first one (H_{sa}), has composition: Ni–45.23Ti wt.%; the second one, (M_{cw}): Ni–44.62Ti wt.%.

In the factory, before being delivered to our laboratory, the H_{sa} was straight annealed (sa) at 450 °C for 1 h and has a martensite to austenite transition peak temperature (A_p), equal to 91 °C (see below).

As discussed in the paper, the different surface conditions induced by the thermomechanical treatments, including composition changes of the outer layers of the two materials, are playing a major role in determining the observed results. Nevertheless, the different compositions of the selected alloys have been observed to induce detectable differences in the reported results.

The cold-worked (cw) M_{cw} alloy was not recovered after drawing and, therefore, it was still strain hardened when used in our experiments. The hardened condition stabilises the austenite phase down to –50 °C. All thermal data, provided with the product technical data sheet, have been actually confirmed by differential scanning calorimetry (DSC) tests we carried out on our own to measure all relevant transition temperatures. In particular, the M_{cw} material remained austenitic down to cryogenic temperatures. As concerns the H_{sa} alloy, the following transition temperatures were measured, to confirm the product specifications:

Martensite start (M_s)=45 °C
 Martensite finish (M_f)=29 °C
 Austenite start (A_s)=87 °C
 Austenite finish (A_f)=99 °C

Therefore, from DSC results we can conclude that, as expected, at room temperature the H_{sa} and the M_{cw} alloys are martensitic and austenitic, respectively.

Two kinds of surface treatments have been selected, after cleaning the surface of the wire specimens with acetone in an

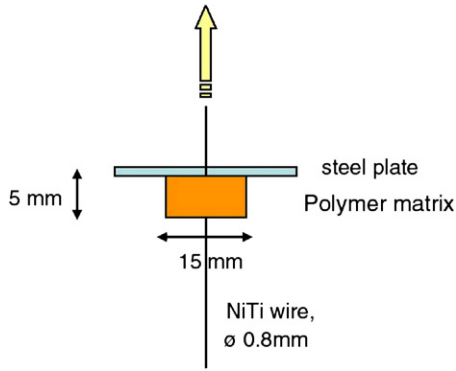


Fig. 1. schematic drawing of pull out test geometry.

ultrasonic bath. The first one is a purely mechanical modification of the alloy surface. The other consists of three separate chemical treatments, involving the immersion of wire specimens in both acidic and basic solutions.

The mechanical treatment consists in abrading the original surface with 180 and 400 grit papers.

As concerns chemical treatments, three procedures have been followed:

A-treatment: 2 h in a 32.5% nitric acid water solution at 80 °C [33].

AB-treatment: A-treatment followed by a 4 hour dipping in a basic 1.2 M NaOH aqueous solution (pH~ 14) at 80 °C [33].

The ABA-treatment consists in an AB-treatment followed by a 30 min. immersion in a 32.5% nitric acid water solution kept at 80 °C (± 2 °C). Temperature was carefully controlled not to induce the martensite to austenite transition in the H_{sa} alloy.

After each chemical treatment the samples were rinsed in demineralised water and dried at room temperature.

The original and the treated surfaces were analysed using optical and environmental scanning electron microscope ESEM-TMP FEI (secondary electron images were obtained in low vacuum mode). The ESEM was equipped with an energy dispersive x-ray spectrometer (EDXS) used for qualitative microanalysis of the investigated regions.

For the characterisation of corrosion behaviour, induced by these surface treatments, electrochemical tests in 1 wt.% NaCl aerated solution were carried out. A three-electrode electrochemical cell is used with a Ag/AgCl (+207 mV SHE) reference electrode and a platinum grid counter-electrode. An EG&G 273 potentiostat connected to a frequency analyser FRA Solartron 1260 and a PC were used.

Potentiodynamic polarization tests were performed using a polarization rate of 0.5 mV/s, starting from cathodic potentials (from -600 to 1500 mV vs. Ag/AgCl).

Electrochemical Impedance Spectroscopy (EIS) measures were carried out with a signal amplitude of 10 mV, in the frequency range of 100 kHz and 1 mHz at free corrosion potential [35,36]. EIS data were worked out with an Equivrt software, developed by Boukamp [37].

For each sample we repeated the electrochemical measurements three times in order to verify the reproducibility of the experimental approach.

To evaluate the influence of surface treatments on the alloy adhesion to a polymeric matrix, pull-out tests were conducted. These tests are commonly used to evaluate the adhesion strength between fibre and matrix in composite materials [31,32]. According to the test geometry used by Smith et al. [7] and K. Lau et al. [6], a single SMA wire was embedded into an epoxy resin cylinder for a length of 5 mm. A schematic drawing of the geometry of the test is shown in Fig. 1. Mechanical tests (pull out) on the SMA wires and epoxy matrix were performed with an Instron (model 4501) universal testing machine. A metallic sheet with a 1 mm diameter hole was used to load the epoxy matrix. A loading rate of 0.1 mm/min was used in order to avoid dynamic effects and the occurrence of cracks away from the wire/matrix interface. To have a significantly wide data set, eight specimens for each sample were tested.

A commercial bi-component epoxy matrix (EC57/K21), supplied by Camattini (Collecchio, Parma, Italy), was employed. The resin consists of a DGEBA-based low molecular weight epoxy resin (EC57: epoxy-equivalent 172–182 g/equiv) and a penta-ethylene-hexamine curing agent (K21) added to a ratio of 20 phr. A two step curing was carried out at room temperature for 24 h and at 80 °C for 15 h. Eventually, the resin had a tensile

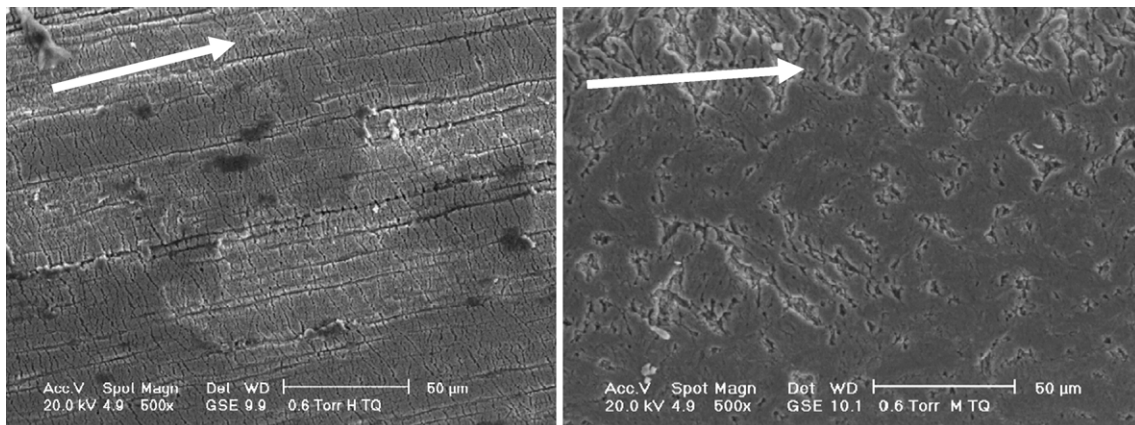


Fig. 2. Surface morphology of untreated NiTi wires: H_{sa} (left) and M_{cw} (right). Arrows indicate the drawing direction.

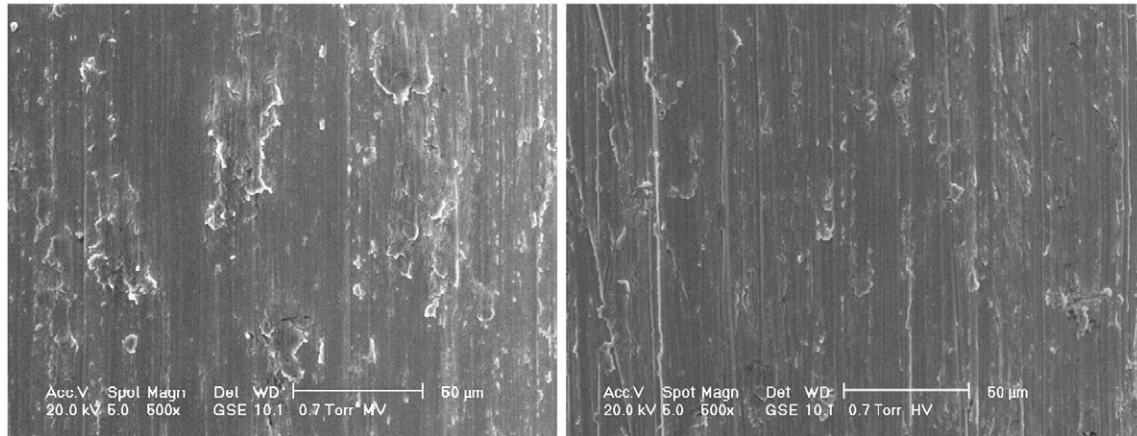


Fig. 3. Surface morphology of mechanical abraded NiTi wires: H_{sa} (left) and M_{cw} (right).

modulus of 1.82 ± 0.06 GPa, a strength (σ_r) of 66 ± 2 MPa, and a rupture strain (ϵ_r) of $6.2 \pm 0.8\%$.

3. Results and discussion

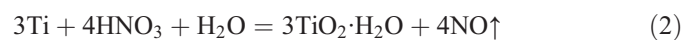
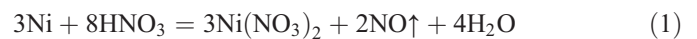
3.1. Microstructural analyses

The H_{sa} alloy wires, in the as-delivered condition, have an extremely heterogeneous surface morphology (Fig. 2), most likely resulting from the oxidation reactions occurring during the (straight) annealing treatments. Several microcracks, mainly normal to the drawing direction, have been observed. They are probably determined by an exceedingly high surface drawing strain in the alloy and to the thermal stresses building up in the oxide layer. EDXS analyses indicate that thermal annealing resulted in a titanium depletion in the outer surface layer of the alloy, beneath the oxide, with a consequent nickel enrichment, due to the outward migration of titanium to form an oxide layer [38].

Quite a different surface morphology has been observed on the M_{cw} wires (Fig. 2). Their topography appears more uniform and without an extensive micro-cracking, probably for a more limited oxidation.

The mechanical polishing treatment removes most of the defects described above, and the two alloys, H_{sa} and M_{cw} , display quite a similar surface aspect, as shown by the micrographs in Fig. 3.

The acid treatment (A) removes the native oxide layer and starts corroding the alloy surface (Fig. 4). Oxidation proceeds through alternating steps, during which titanium and nickel are preferentially reacting with the etching solution [33]. A selective alloy corrosion occurs, with nickel going into solution, whereas titanium is preferentially oxidised and remains as an adherent oxide layer. The relevant reactions are the following [34]:



The resulting reaction layer building up on the alloy surface is rather porous [33], a feature that might be beneficial to increase matrix adhesion, even if this can have a negative effect on surface chemical stability of the alloy, that results not to be fully protected against possible further corrosion attacks. Although the general microstructural features of the reaction layer seem not to be dependent on the underlying alloy, as

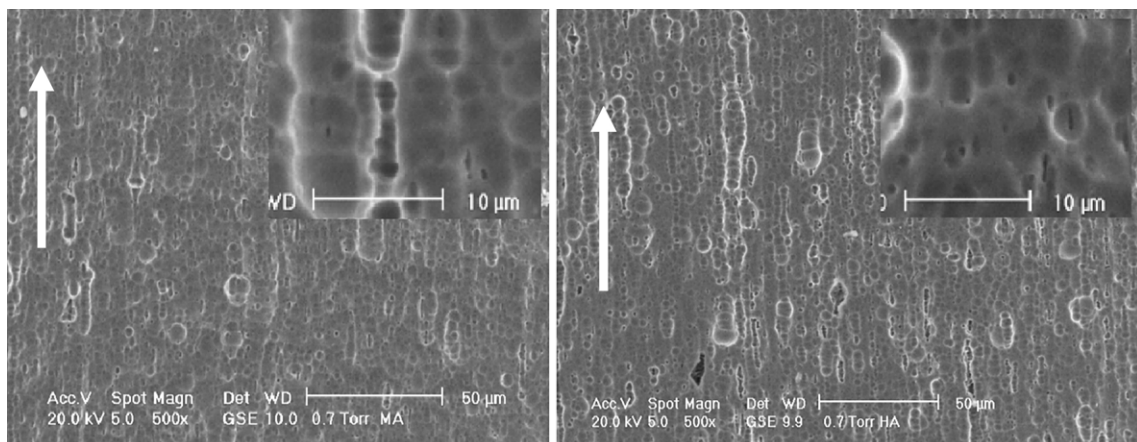


Fig. 4. Surface morphology of NiTi wires after acid treatment (A): H_{sa} (left) and M_{cw} (right). Arrows indicate the drawing direction. Insets: higher magnification images.

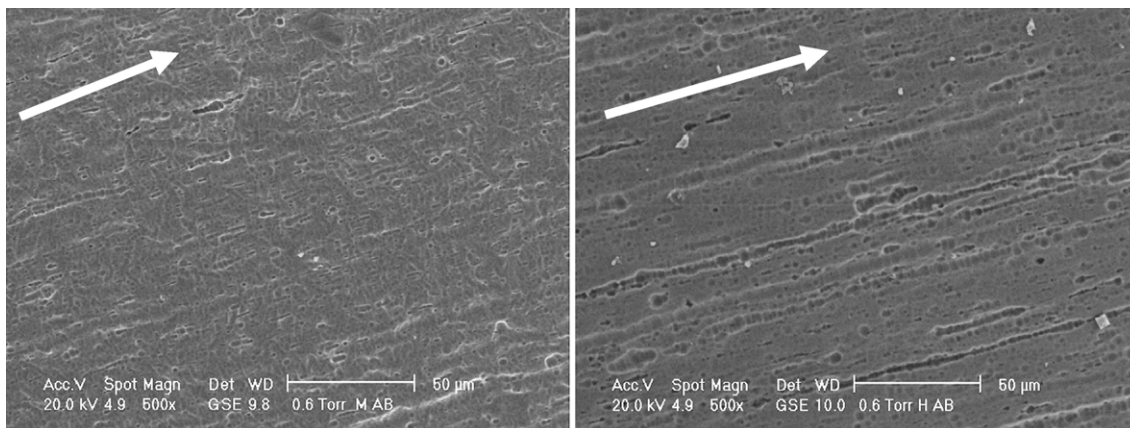


Fig. 5. Surface morphology of NiTi wires after acid–basic treatment (AB): H_{sa} (left) and M_{cw} (right). Arrows indicate the drawing direction.

concerns porosity, the H_{sa} material displays larger pores than those that formed on the M_{cw} alloy, as resulted from microscopy observations carried out at higher magnifications. This difference is compatible with a higher reactivity that can be assumed for the H_{sa} alloy, that, as previously mentioned, has a nickel rich outer surface layer.

A completely different surface morphology has been observed on the alloy samples treated with the basic solution also (AB treatment, Fig. 5). In this case the solution transforms titanium oxide, that formed during the A-treatment (see Eq. (2)), into a hydrated, porous titanium oxide [33]. Consequently, nickel can preferentially react with the basic solution, according to the following reaction:



The H_{sa} material shows a coarser and more interconnected porosity than the one observed after acid treatment. The M_{cw} alloy displays a corrugated surface with traces of pitting corrosion.

Eventually, after a further immersion of the wires into the acid solution (ABA treatment), the surface topographies of the two alloys remains in very similar conditions as those observed after the AB treatment. From the relevant SEM micrographs it is

possible to note qualitatively that the M_{cw} alloy displays a rougher surface than H_{sa} alloy, particularly along the drawing direction (Fig. 6).

3.2. Free corrosion potential, $E_{corr}(t)$

Figs. 7 and 8 display the evolution with time of the free corrosion potentials for the samples of both alloys in the as-received conditions and after the different surface treatments. The reproducibility of the measurements was good and the reported plots are representative of the general behaviour of the samples.

The H_{sa} alloy (Fig. 7) displays a more cathodic behaviour than the M_{cw} wire (Fig. 8), irrespective of the surface condition, with an E_{corr} value close to that of pure nickel. The as-received H_{sa} material displays a sharp decrease in the E_{corr} vs. time curve, that is most likely to be associated to the sudden activation of a localised corrosion due to a defective oxide surface layer. On the other hand, the E_{corr} vs time curve for the H_{sa} alloy has quite an irregular trend, that is due to the difficulty for the alloy to form a continuous and dense oxide layer on its very rough and irregular surface. Contrarily, the as-received M_{cw} alloy shows a more regular behaviour in the potential curve, that is comparatively

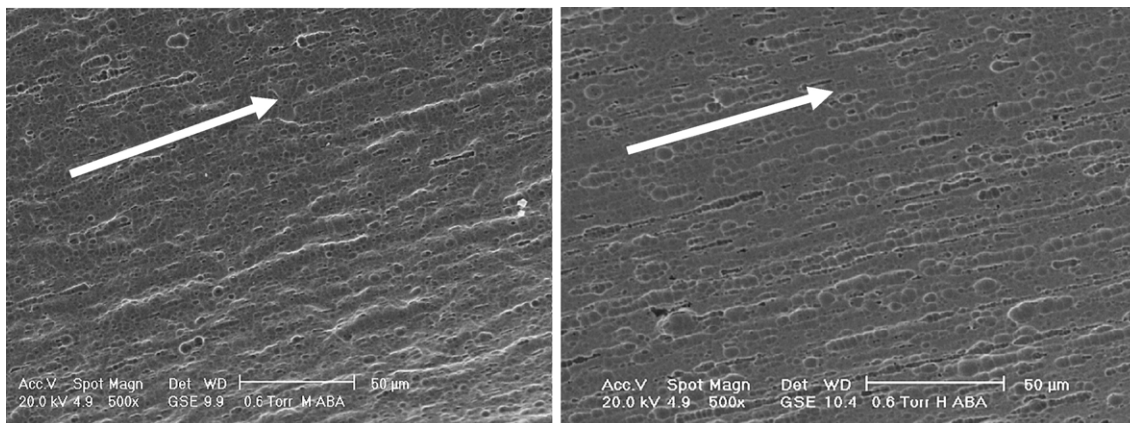


Fig. 6. Surface morphology of NiTi wires after acid–basic–acid treatment (ABA): H_{sa} (left) and M_{cw} (right). Arrows indicate the drawing direction.

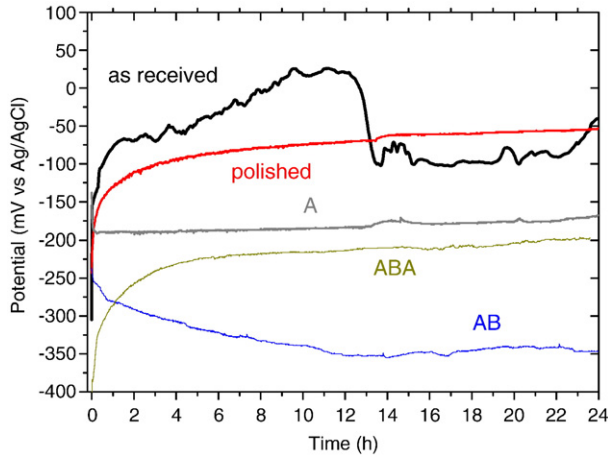


Fig. 7. Free corrosion potential vs. time of H_{sa} alloy, as a function of the surface treatments.

more stable over the considered time span thanks to the presence of a more protective layer of titanium oxides.

All samples that have been mechanically polished, so that most of the oxides originally present on their surface have been removed, display very stable E_{corr} values. The M_{cw} alloy confirms its lower nobility (more cathodic behaviour) than H_{sa} , although both alloy materials, once they have been mechanically treated, display a more stable behaviour, as compared to their initial as-received conditions, thanks to the formation of a more uniform passivation oxide layer.

After the A-treatment, the M_{cw} alloy turns to be more noble than the H_{sa} alloy for a short period (1 h), although the relevant curves show very close values for longer times. This effect can be ascribed to two competitive phenomena occurring at the surface of each alloy during the A-treatment: the oxidation of the M_{cw} , with the growth of a TiO_2 -rich scale and a preferential removal of nickel, that is brought into solution, from the surface of H_{sa} alloy.

The AB-treatment results in a drastic reduction of the corrosion potentials for both alloys, indicating a higher reactivity

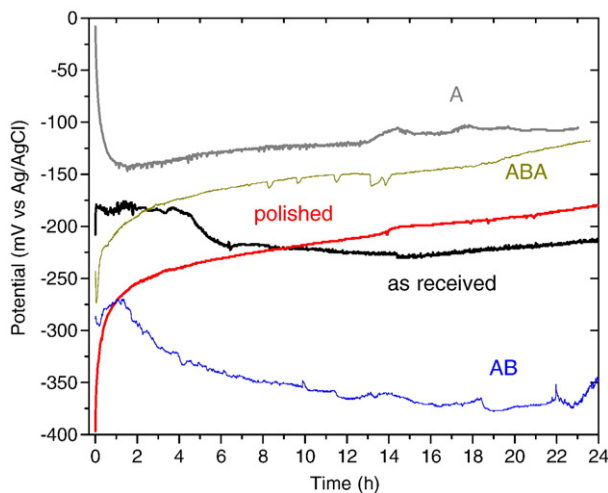


Fig. 8. Free corrosion potential vs. time of M_{cw} alloy, as a function of the surface treatments.

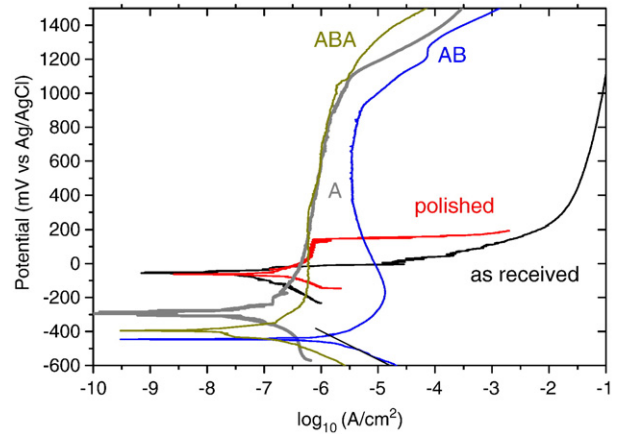


Fig. 9. Polarization curves for the H_{sa} alloy after different surface treatments.

of these materials induced by the removal of the pre-existing titanium oxide passivation layer.

The ABA-treatment sets the potentials back to the values they had after the A-treatment, as the second dipping into the acid solution induces the new formation, a little more pronounced in the M_{cw} material, of the oxide layer dissolved by the previous basic treatment. Although corrosion potentials of the ABA-treated alloys are close to the values of the A-treated samples, their surface results to be quite different (Fig. 6).

3.3. Polarisation curves

The polarisation curves, representative of the typical behaviour of each surface condition, are displayed in Figs. 9 and 10. From the graphs it turns out that the H_{sa} material does not display any passivation behaviour because of the unprotective thermal oxide.

From Figs. 9 and 10 it is also possible to get information concerning the corrosion current (i_{corr}), by considering the geometrical intercepts of the Tafel slopes, which are the slope of the cathodic and anodic curves close to the free corrosion potential.

The M_{cw} alloy has rather low anodic currents in the passivity interval, compatible with a passivity regime occurring before the breakdown potential, (0.23 V vs Ag/AgCl).

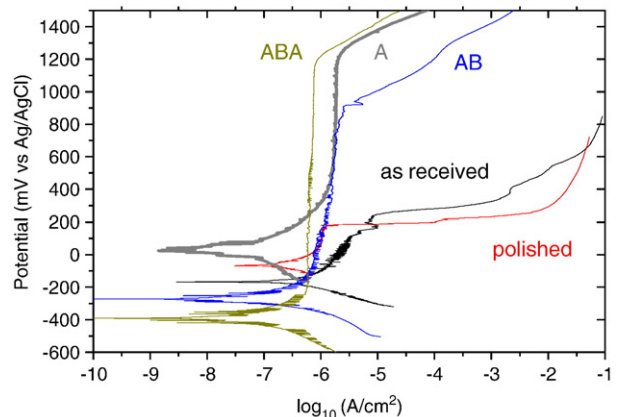


Fig. 10. Polarization curves for the M_{cw} alloy after different surface treatments.

The mechanical polishing treatment is not significantly affecting the i_{corr} values of the M_{cw} alloy with respect to the as-received condition. In the case of the H_{sa} alloy, i_{corr} is increasing by one order of magnitude nearly, because of the spalling off of native oxide layer, that is initially present on the surface of the samples. In this way, clean alloy surfaces are exposed to air and become immediately covered with a thin passivating oxide scale. However, owing to the limited thickness of the native oxide layer growing on the M_{cw} material, the breakdown potential retains values as high as those of the untreated, i.e., unpolished, alloys. After the acid treatment (A), the two alloys show a typical passive behaviour, with a large increase in the breakdown potential (1.00–1.20 V vs Ag/AgCl). A remarkable decrease of the corrosion current of the M_{cw} alloy, as compared to the as-received value, is observed. A different situation is observed in the H_{sa} alloy. In the as-received condition a limited current density resulted from the elevated thickness of the original native oxide, whereas in the A-treated material the growth of a thinner layer of TiO_2 results in a minor reduction in the corrosion current, i_{corr} .

From the polarisation curves of the AB-treated alloys, it turns out that the breakdown potential is below 1.00 V vs Ag/AgCl for both materials. A significant increase in i_{corr} is recorded, particularly in the H_{sa} alloy. It is worth noting that in the anodic branch of the curve for the H_{sa} material a typical active to passive transition is present, with passivity currents that retain higher values than in the just A-treated alloy specimens. A similar active to passive transition is not present or, at least, not so evident in the M_{cw} alloy.

The ABA-treatment is the most effective in protecting the alloy in terms of current density and breakdown potential. Indeed, the M_{cw} alloy results to have the lowest current densities and a breakdown potential with values in excess of 1.20 V Ag/AgCl, as those measured for the A-treated alloys. The H_{sa} alloy too displays an increase in the breakdown potential and in the passivity currents, that again are quite close to the data of the A-treated specimens.

3.4. Electrochemical impedance spectroscopy

From the impedance tests additional information on the electrochemical behaviour of the alloys after different surface

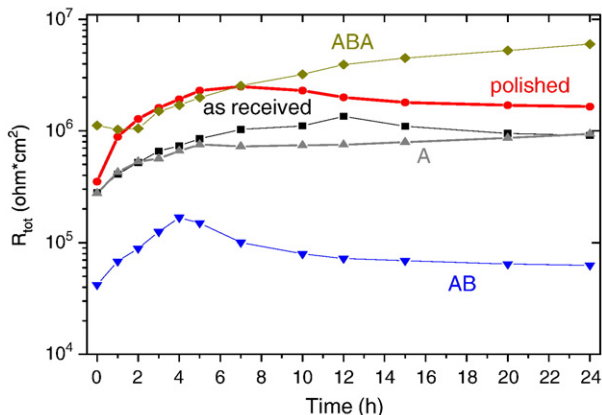


Fig. 11. Total resistance vs dipping time curves for the surface treated H_{sa} alloy.

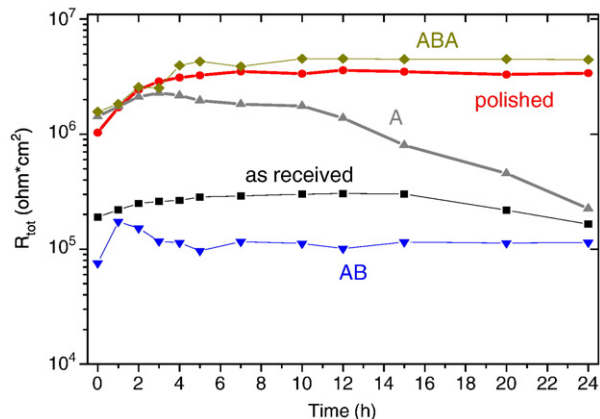


Fig. 12. Total resistance vs dipping time curves for the surface treated M_{cw} alloy.

treatments can be obtained and, thereby, indications on their surface conditions. For the interpretation of the experimental results, that are usually determined by complex reactions, several models are available taking into account all components of the cell impedance [39]. A comparison among samples having different specific features can be made using an equivalent electrical circuit, in which all contributions to electrical resistivity of the cell are grouped into one single term, named total resistance, R_{tot} . This resistive element is assumed to be connected in parallel with a constant phase element. This term is intended to model the impedance contribution due to no ideal capacitive components, like the double layer capacitance on irregular surfaces. In this picture, R_{tot} provides a good indication of the material corrosion resistance [35]. This parameter is influenced and particularly sensitive to the presence and to the kind of surface oxides. The reproducibility of the EIS data was good and reported data are mean values of at least three measurements.

Figs. 11 and 12 display the evolution of R_{tot} with dipping time in the sodium chloride solution. In the as-received condition, the M_{cw} alloy has R_{tot} values lower than those for the H_{sa} alloy. This was to be expected in view of a thicker and not protective oxide scale that formed on the H_{sa} wire during annealing treatments. The H_{sa} alloy not only shows higher resistance values, but also their slight increase with the immersion time. This trend is in agreement with the observed progressive increase in the nobility of the material (Fig. 7). As to the M_{cw} alloy, its resistance remains constant and then decreases, owing to a partial dissolution of the outer passivation layer (Fig. 8).

With the mechanical polishing treatment, the evolution of R_{tot} perfectly follows that of the free corrosion potentials. The R_{tot} values are comparatively higher, namely for the M_{cw} alloy, as wide passivation zones are observed. Therefore, once the oxide surface layer has been mechanically removed, both alloys behave better as regards corrosion resistance for the formation of an extremely protective oxide scale. The values of the resistance for the two alloys are very close, as abrasion is capable to remove the original surface layers and allows for a direct interaction between the solution and the alloys, whose composition is nearly the same.

As concerns the alloys treated in nitric acid (A-treatment), it can be noticed that the M_{cw} material features a significant

increase in the total resistance, comparable, during the early immersion hours, to the values achieved through mechanical polishing treatments. Differently from this behaviour, the H_{sa} alloy has resistance values that are equal to or lower than those measured in the original state. However, while the resistance of the H_{sa} material remains nearly constant over a time span of 24 h, the resistance of the M_{cw} alloy decreases by one order of magnitude nearly over the same period of time, showing a lower stability of the surface layer.

The lower corrosion resistance displayed by the alloy samples treated in the basic solution (AB treatment), as compared to the specimens treated in acid (A treatment), has been confirmed by the impedance spectroscopy tests, that provide total resistivity values as low as $100 \text{ k}\Omega\text{cm}^2$ for the two alloys. This value is at least one order of magnitude below the impedance measured for all other alloy specimens. This behaviour can be justified by the transformation of the oxides into hydrated oxides, that are generally far less protective than the parent oxides. In this case too, the alloy that shows the highest resistivity reduction, as compared to the original value, is the H_{sa} , that is protected by the thermal oxide present on its surface in the as-delivered condition. The ABA treatment is very effective in improving the overall corrosion behaviour of the alloys. The resistance values turn to be the highest among those of all the other treated samples and this can be seen as the result of a complete re-oxidation of the alloy surface. This better corrosion behaviour is in agreement with the findings of the potentiodynamic tests. Thanks to this treatment it has been possible to have corrosion resistant alloys with low values of i_{corr} , high breakdown potentials and resistance to electrical polarisation.

3.5. Pull-out adhesion test

Assuming that the shear stress is uniformly distributed along the resin-embedded length, the mean value of the interfacial shear strength, τ_{ISS} , of the fibre-matrix interface can be written as [40]:

$$\tau_{ISS} = \frac{P_d}{\pi \cdot \phi \cdot l_e}$$

where ϕ and l_e are the diameter and the embedded length of the wire respectively, and P_d the maximum force corresponding to the pull-out process.

Fig. 13 shows the τ_{ISS} values observed for the as-received and the surface treated NiTi wires. The following observations can be made.

The M_{cw} alloy displays higher adhesion properties than the H_{sa} samples in all surface conditions. For the as-received samples this aspect could be attributed to a more uniform and less oxidised surface in the M_{cw} than in H_{sa} sample, in agreement with microscopy observations (Fig. 2).

The AB treatment produces the worse adhesion properties for both alloys. The possible presence of titanium hydroxides on their surface, as inferred from electrochemical characterisation, may reduce the adhesion strength of the epoxy matrix to the alloy wires. Moreover, the poor mechanical properties

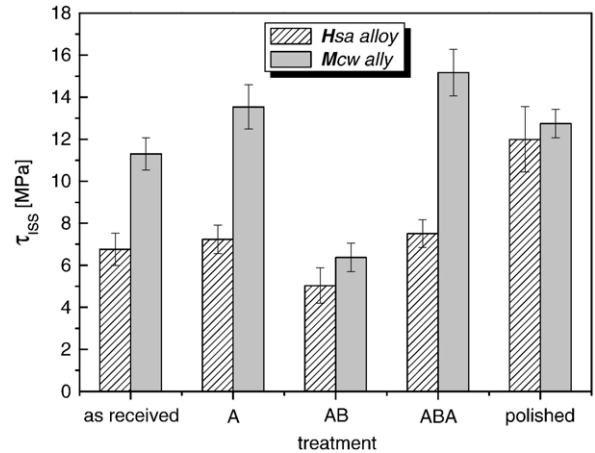


Fig. 13. Mean interface shear strength of the wire-resin interface for different surface conditions.

of the titanium hydroxide layer weaken the overall wire-matrix adhesion strength.

In the H_{sa} alloy, the mechanical polishing treatment produces the best adhesion properties. The good performance produced in the H_{sa} and M_{cw} materials by mechanical polishing would recommend an optimisation of this treatment, using, for instance, a micro sandblasting [31].

It is worth noticing that mechanical polishing resulted to be the only surface treatment that improves the pull-out performance of the H_{sa} alloy embedded in the resin. This alloy in all the other conditions, including the original one, displays lower and nearly constant values of the interfacial shear strength.

The A and ABA treatments increase the adhesion properties of the M_{cw} alloy as the acid solution produces uniform corrosion attacks, that render wire surface more regular and, therefore, more homogeneously covered by the resin. Despite the different surface topography of the ABA surface, with a higher roughness in comparison with the A treatment, there are limited differences in the pull-out results, leading to the conclusion that, for our system, the complex ABA treatment is not justified.

In all conditions, pull-out stresses for the M_{cw} alloy are far below the typical values for austenite–martensite transition stresses for NiTi alloys (minimum values about 200 MPa). For this reason no mechanical induced transition would occur during the pull-out tests.

4. Conclusions

Quite different surface morphologies were obtained from different surface treatments carried out on two different NiTi alloy wires. The more protective oxide surface layer of H_{sa} alloy beneficially affects the corrosion resistance of this alloy, that performs better than the M_{cw} material. The native passivating oxide layers, that forms in air, have a limited corrosion protection capacity, as proved by the low breakdown potential.

The treatment in nitric acid removes the surface passive layer and promotes a selective corrosion, that preferentially dissolves nickel and fully oxidise titanium. The resulting surface layers are

definitely more protective and result in an excellent corrosion behaviour of the alloys. The treatment in the basic solution turns titanium oxide into hydrated compounds increasing the concentration of Ti–OH groups on the surface. Consequently, both H_{sa} and M_{cw} alloys result to have a lower corrosion resistance. Therefore a further acid treatment has to be carried out afterward in order to re-establish a passivity condition, that optimises the corrosion resistance of the alloys.

Considering the adhesion between wires and polymeric matrix, the M_{cw} alloy displays better properties than the H_{sa} samples in all surface conditions.

As to the M_{cw} alloy the A and ABA treatments produce the best performances determined by a better quality of the oxide scales resulting from these treatments. Nevertheless, considering the very little differences in the performances of A and ABA treatments, the simplest approach, i.e., the A-treatment, is to be preferred. This is not so for the H_{sa} samples, as in this case mechanical polishing produces the best performance.

The basic treatment (AB) decreases drastically the adhesion properties due to the formation of Ti hydroxide species on the surface of both materials.

References

- [1] K. Otsuka, C.M. Wayman, Shape memory materials, Cambridge University Press, Cambridge UK, 1998.
- [2] K. Lau, A.W. Chan, S. Shi, L. Zhou, Mater. Des. 23 (2002) 265.
- [3] N.A. Smith, G.G. Antoun, A.B. Ellis, W.C. Crone, Compos., Part A Appl. Sci. Manuf. 35 (2004) 1307.
- [4] B.K. Jang, T. Kishi, Mater. Lett. 60 (2006) 518.
- [5] G. Rondelli, Biomaterials 17 (1996) 2003.
- [6] P. Roche, L. El Medawa, J.-C. Hornez, M. Traisnel, J. Brems, H.F. Hildebrand, Scr. Mater. 50 (2004) 255.
- [7] H.C. Lin, S.K. Wu, T.S. Chou, H.P. Kao, Acta Metall. Mater. 39 (1991) 2069.
- [8] Y. Liu, D. Favier, Acta Mater. 48 (2000) 3489.
- [9] W.D. Armstrong, H. Lilholt, Mater. Sci. Eng., B, Solid-State Mater. Adv. Technol. 68 (2000) 149.
- [10] B.K. Jang, T.T. Kishi, Mater. Lett. 59 (2005) 2472.
- [11] M. Es-Souni, M. Es-Souni, H. Fischer-Brandies, Biomaterials 23 (2002) 2887.
- [12] P. Sittner, R. Stalmans, JOM 52 (2000) 15.
- [13] A.J. Kinloch, Adhesion and adhesives: science and technology, Chapman & Hall, London (UK), 1987.
- [14] C. Trigwell, T. Duerig, Surf. Interface Anal. 15 (1990) 349.
- [15] N.A. Smith, G.G. Antoun, A.B. Ellis, W.C. Crone, Compos., Part A Appl. Sci. Manuf. 35 (2004) 1307.
- [16] H.C. Man, K.L. Ho, Z.D. Cui, Surf. Coat. Technol. 200 (2006) 4612.
- [17] Z.D. Cui, H.C. Man, X.J. Yang, Surf. Coat. Technol. 192 (2005) 347.
- [18] F. Villermaux, M. Tabrizian, L. 'H. Yahia, M. Meunier, D.L. Piron, Appl. Surf. Sci. 109/110 (1997) 62.
- [19] Z.D. Cui, H.C. Man, X.J. Yang, Appl. Surf. Sci. 208–209 (2003) 388.
- [20] H.C. Man, N.Q. Zhao, Surf. Coat. Technol. 200 (2006) 5598.
- [21] H.C. Man, N.Q. Zhao, Appl. Surf. Sci. 253 (2006) 1595.
- [22] N.Q. Zhao, H.C. Man, Z.D. Cui, X.J. Yang, Surf. Coat. Technol. 200 (2006) 4879.
- [23] C. Trepanier, T.K. Leung, M. Tabrizian, L. Yahia, J.G. Bienvenu, J.F. Tanguay, D.L. Piron, L. Bilodeau, J. Biomed. Mater. Res. 43 (1998) 165.
- [24] X. Ju, H. Dong, Surf. Coat. Technol. 2001 (2006) 1542.
- [25] R.W.Y. Poon, K.W.K. Yeung, X.Y. Liu, P.K. Chu, C.Y. Chung, W.W. Lu, K.M.C. Cheung, D. Chan, Biomaterials 26 (2005) 2265.
- [26] R.W.Y. Poon, J.P.Y. Ho, X. Liu, C.Y. Chung, P.K. Chu, K.W.K. Yeung, W.W. Lu, K.M.C. Cheung, Nucl. Instrum. Methods Phys. Res., B Beam Interact. Mater. Atoms 237 (2005) 411.
- [27] R.W.Y. Poon, J.P.Y. Ho, C.M.Y. Luk, X. Liu, J.C.Y. Chung, P.K. Chu, K.W.K. Yeung, W.W. Lu, K.M.C. Cheung, Nucl. Instrum. Methods Phys. Res., B Beam Interact. Mater. Atoms 242 (2006) 270.
- [28] R.W.Y. Poon, J.P.Y. Ho, X. Liu, C.Y. Chung, P.K. Chu, K.W.K. Yeung, W.W. Lu, K.M.C. Cheung, Thin Solid Films 488 (2005) 20.
- [29] S. Mändl, A. Fleischer, D. Manova, B. Rauschenbach, Surf. Coat. Technol. 200 (2006) 6225.
- [30] H. Pelletier, D. Muller, P. Mille, J.J. Grob, Surf. Coat. Technol. 158–159 (2002) 301.
- [31] K. Jonnalagadda, G.E. Kline, N.R. Sottos, Exp. Mech. 37 (1) (1997) 78.
- [32] J.S.N. Paine, W.M. Jones, C.A. Rogers, AIAA; 33rd Structural Dynamics and Materials Conference, 1992, p. 556.
- [33] M.F. Chen, X.J. Yang, Y. Liu, S.L. Zhu, Z.D. Cui, H.C. Man, Surf. Coat. Technol. 173 (2003) 234.
- [34] M. Pohl, C. Heßing, J. Frenzel, Mater. Sci. Eng., A Struct. Mater.: Prop. Microstruct. Process. 378 (2004) 191.
- [35] J. Ross Macdonald, Impedance spectroscopy: emphasizing solid materials and systems, Wiley, New York (USA), 1987.
- [36] J.R. Scully, Electrochemical impedance: analysis and interpretation, American Society for Testing and Materials, Philadelphia, USA, 1993.
- [37] B. Boukamp, Solid State Ionics 20 (1986) 31.
- [38] B. O'Brien, W. Carroll, J. Kelly Biomater. 23 (2002) 1743.
- [39] S. Rossi, L. Fedrizzi, T. Bacci, G. Pradelli, Corros. Sci. 45 (2003) 511.
- [40] B. Miller, U. Gaur, D.E. Hirt, Compos. Sci. Technol. 42 (1991) 207.